

The Gardner transition in physical dimensions

C. L. Hicks, M. J. Wheatley, M. J. Godfrey, and M. A. Moore

School of Physics and Astronomy, University of Manchester, Manchester M13 9PL, UK

(Dated: June 15, 2018)

The Gardner transition is the transition that at mean-field level separates a stable glass phase from a marginally stable phase. This transition has similarities with the de Almeida-Thouless transition of spin glasses. We have studied a well-understood problem, that of disks moving in a narrow channel, which shows many features usually associated with the Gardner transition. We show that some of these features are artifacts that arise when a disk escapes its local cage during the quench to higher densities. There is evidence that the Gardner transition becomes an avoided transition, in that the correlation length becomes quite large, of order 15 particle diameters, even in our quasi-one-dimensional system.

In a remarkable series of papers (see Ref. [1] for a review and references) the large-dimension limit of the hard sphere fluid has been solved. This program of calculation provides the mean-field description relevant for the dynamical glass phase transition, the Kauzmann ideal glass transition, the Gardner transition and the geometrical description of the properties of jammed states. The next step is of course to understand what happens in finite dimensions. In this paper we argue that at least the Gardner transition is not a real transition in physical dimensions, $d \leq 3$. The Gardner transition is the transition associated with the emergence of a complex free-energy landscape composed of many marginally stable sub-basins contained within a larger glass metabasin [2]. It is thus similar to a state of a spin glass in a phase with broken replica symmetry [3]. In fact the field theory of the Gardner transition is closely related to that of the Ising spin glass problem in a random magnetic field – the de Almeida-Thouless transition [4].

It has been argued for some time that the de Almeida-Thouless transition only occurs in systems with dimensions $d > 6$ [5–7], but this is still controversial [8–11]. Furthermore in two dimensions there is not even a spin glass transition in zero field, and none has been detected either in a finite field. Nevertheless, both simulations [12] and experiments on hard disks in two dimensions [13, 14] seem to provide evidence for a Gardner transition during compression; i.e., that glass systems that start with the same particle positions but with different particle velocities, can, by the end of the compression, be in mutually inaccessible states. To understand what might be going on, we have applied the methods of Ref. [12] to a system of hard disks moving in a narrow channel, which is a model that has previously been studied in some detail [15–25]. Our system, being one dimensional, cannot have a true phase transition. We find that we can produce the same kinds of behavior that other investigators studying two- and three-dimensional hard sphere systems have explained in terms of the state-following Gardner transition. However, because of the simplicity of our system we can give a full explanation of our observations. We find that some of the behavior that has been ascribed to the Gardner transition (such as a nontrivial change in the distribution of an order parameter) arises when the

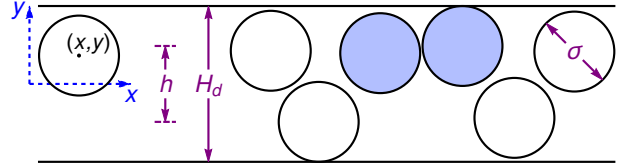


FIG. 1. (Color online) The system of hard disks in a channel. The distance H_d is the width of the channel, σ is the diameter of each disk, and $h = H_d - \sigma$ is the width of the channel accessible to the centers of the disks. For the coordinates (x, y) of the disk, y is measured from the center line of the channel. The blue shaded disks can be regarded as a *defect* in the zigzag arrangement of the disks that is favored at high density.

time scales associated with the quench used in the state-following investigations are long enough for there to be a significant chance of a disk escaping its cage by crossing the channel. Our results thus do not imply that there are glasses that are stable and glasses that are marginal, with the Gardner transition separating the two [12]. Effects that have been attributed to the Gardner transition in two- and three-dimensional hard-sphere systems may also have a simple explanation, connected with just a few disks or spheres escaping their cages on the time scale of the quench. In a recent preprint, Scalliet et al. [26] have invoked a similar mechanism to help explain the absence of a Gardner transition in a system of particles that interact via a soft potential. However, for our system of hard disks we can provide evidence that there is an avoided Gardner transition at which the correlation length grows to a large value, ≈ 15 particle diameters, but does not diverge. For hard spheres in three dimensions, which is closer to the mean-field limit of infinite dimension, we suspect that the equivalent length scale will be larger still and exceed the linear dimensions of the systems that were simulated [12], making it impossible to distinguish a true phase transition from an avoided one.

Details of the system that we are studying are given in Fig. 1. The packing fraction ϕ is defined as $\phi = N\pi\sigma^2/(4H_dL)$, where N is the number of disks in a chan-

nel of length L . The channel width H_d was taken to be 1.95σ , where σ is the diameter of a disk; we have previously made extensive transfer-matrix [27] calculations of thermodynamic properties and correlation functions for this case [16].

The dynamics in this system start to slow as “zigzag” order sets in above a packing fraction $\phi = \phi_d \approx 0.48$ [15–17]. This kind of order is characterized by successive values of y_i taking opposite signs (see Fig. 1). The zigzag order can be interrupted by defects where successive y_i are of the same sign; the correlation length ξ for zigzag order is approximately half the average distance between defects [17]. These defects play an important role in our analysis of the dynamics of the system. (Defects of one kind or another seem to play an important role across the whole of glass physics [28–31].) Their spacing increases rapidly with increasing ϕ , such that ξ passes 2000 at $\phi = 0.7206$ and reaches $\xi = 2.3 \times 10^6$ at $\phi = 0.76$.

We use event-driven molecular dynamics for our simulations. The number of disks N is taken to be 4000 and periodic boundary conditions are applied in the x -direction. We start the system in an initial “equilibrium” state of packing fraction $\phi_i \geq 0.70$ and use the Lubachevsky-Stillinger algorithm [32] to compress it to values of $\phi > \phi_i$ on a time scale much less than the α relaxation time at the packing fraction ϕ_i . We put the word “equilibrium” in quotes as for the packing fractions studied there should be no or very few defects present in the system, but we have found there are typically ~ 10 present, owing to imperfect equilibration. During the compression, the diameter of the disks is increased at a rate $\dot{\sigma}$ and the width of the channel is also increased so that the relation $H_d = 1.95\sigma$ is maintained throughout the compression [19]. Such a compression is “state following” if on the time scale of the quench most of the disks remain caged and do not move far from their initial positions. The kinetic energy of the disks increases during the compression, so, after the quench, the disks are assigned new velocities drawn from a Maxwellian distribution for particles of mass $m = 1$ at a reciprocal temperature $\beta = 1$. The unit of length is chosen so that $\sigma = 1$.

We judge the extent of caging by studying the mean-squared y -displacements (MSD) of the disks from their initial positions $y_i(t_W)$,

$$\Delta(t, t_W) = \frac{1}{N} \sum_{i=1}^N \langle [y_i(t + t_W) - y_i(t_W)]^2 \rangle, \quad (1)$$

averaged over both thermal fluctuations and initial states. The time t starts after a waiting time t_W when the compression has reached a chosen target packing fraction ϕ . The MSD $\Delta(t, t_W)$ grows initially as t^2 from zero at $t = 0$ (see Fig. 2). For our choice of channel width the disks cannot pass each other so the ordering $0 \leq x_1 < x_2 < \dots < x_N < L$ is preserved at all times, and the disks are always caged in the x -direction. Caging in the y -direction is indicated by the presence of a

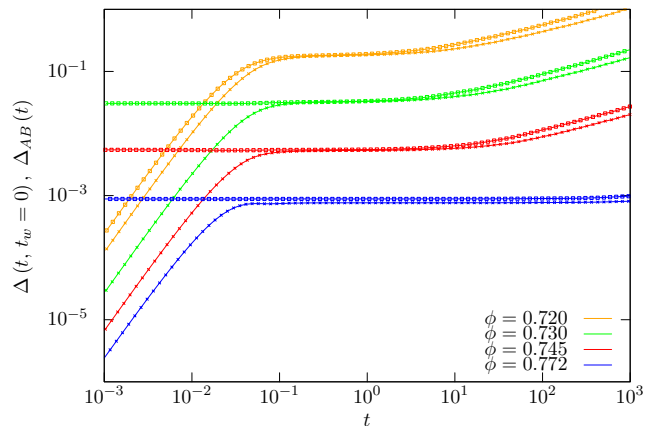


FIG. 2. (Color online) Mean-squared displacements $\Delta(t, t_W = 0)$ [crosses] and $\Delta_{AB}(t)$ [squares] as a function of time t , where the quench was started from the initial “equilibrium” state of packing fraction $\phi_i = 0.720$, which contains defects, and compressed to packing fractions $\phi = 0.730, 0.745$ and 0.772 . Data have been multiplied by 5^k , with $k = 0, \dots, 3$ for $\phi = 0.772, \dots, 0.72$ respectively so the data points do not obscure each other. Note that for $\phi = \phi_i = 0.720$ there was no quench; no disks crossed the channel in this case, so Δ_{AB} follows Δ closely.

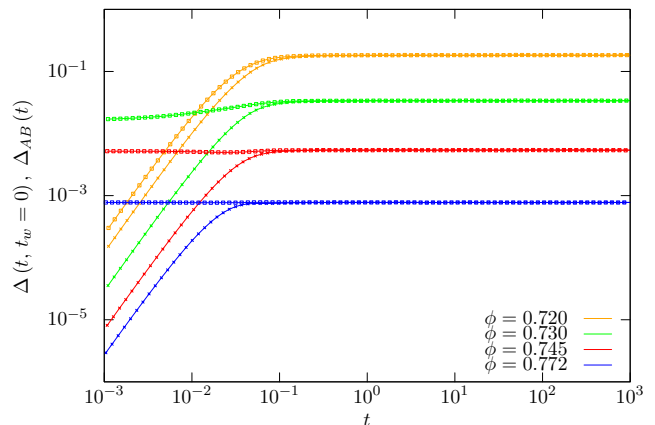


FIG. 3. (Color online) Mean-squared displacements $\Delta(t, t_W = 0)$ [crosses] and $\Delta_{AB}(t)$ [squares] as a function of time t , where the quench was started from an initial state of packing fraction $\phi_i = 0.720$, which contained *no defects*, and compressed to packing fractions $0.730, 0.745$ and 0.772 . Data have been multiplied by 5^k , with $k = 0, \dots, 3$ for $\phi = 0.772, \dots, 0.72$, respectively, so the data points do not obscure each other. Notice that there is no splitting on the plateau between Δ and Δ_{AB} .

plateau in $\Delta(t, t_W = 0)$; the plateau is present for packing fractions $\phi > 0.7$ (see Fig. 2), rather than for $\phi \gtrsim \phi_d$, as seen in two- and three-dimensional systems. Caging is a pre-requisite for seeing the state-following Gardner transition [12]. In contrast to the studies of two- and three-dimensional systems, $\Delta(t, t_W)$ cannot increase indefinitely as $t \rightarrow \infty$ since in our system $|y_i| \leq h/2$. The

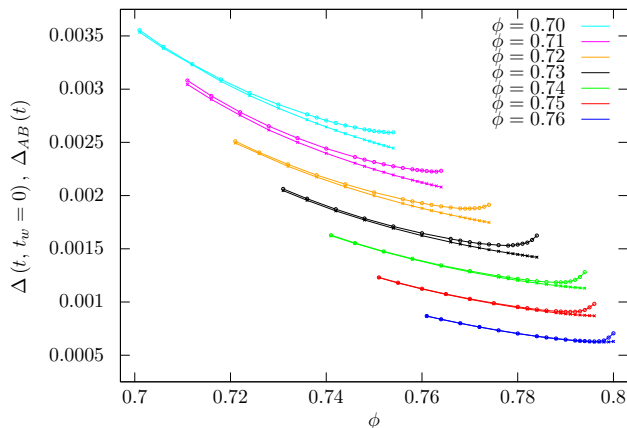


FIG. 4. (Color online) Comparison of the plateau values of Δ and Δ_{AB} for the system with defects showing that the two separate, with $\Delta_{AB} > \Delta$, as ϕ increases. For clarity, the data have been shifted up by $0.00025k$, where $k = 0, 1, \dots, 6$ for $\phi = 0.76, 0.75, \dots, 0.70$, respectively. Error bars are insignificant in comparison to the size of the data points.

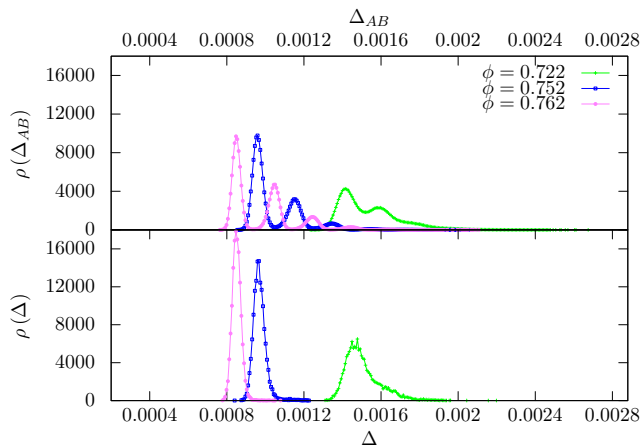


FIG. 5. (Color online) Distribution of plateau values of Δ , $\rho(\Delta)$ and of Δ_{AB} , $\rho(\Delta_{AB})$ following a quench from $\phi_i = 0.71$ to the packing fractions $\phi = 0.722, 0.752$ and 0.762 . The smaller peaks in $\rho(\Delta_{AB})$ are due to one or more disks crossing the channel during the quench.

α relaxation time τ_α is defined as the time at which Δ leaves the plateau, which in our system is the result of disks crossing from one side of the channel to the other; quantitative estimates for τ_α are given in the Supplemental Material [33]. Channel crossing is catalyzed by the presence of the defects; if defects are absent, they must first be nucleated in pairs [15, 16], and this is a process that takes much longer than the α relaxation time [15]. We have prepared initial states free of defects and have found for such states that we cannot observe the end of the plateau on the times for which we could run the simulation; this is shown in Fig. 3. In such systems there is no channel crossing on accessible time scales.

To see Gardner-like behavior, one must study independent copies A and B of the system [12]. Initially, the disks in A and B have identical coordinates (x_i, y_i) , taken from the “equilibrium” state at ϕ_i , but they are assigned different velocities drawn from a Maxwellian distribution. The quantity studied is the MSD of their separation,

$$\Delta_{AB}(t) = \frac{1}{N} \sum_{i=1}^N \langle [y_{A,i}(t) - y_{B,i}(t)]^2 \rangle. \quad (2)$$

In Fig. 2 we show our results for Δ and Δ_{AB} as a function of time for various initial packing fractions. At the larger packing fractions, they show a feature that has been previously been regarded as a signature of the Gardner transition, a difference between the plateau values of $\Delta(t, t_W)$ and $\Delta_{AB}(t)$ [12]. These have been plotted against ϕ in Fig. 4. To extract the plateau values, we used the method of Ref. [12], in which the MSD starting from a given equilibrium state are rescaled to a universal curve of Δ/Δ_m against t/t_m , where Δ_m and t_m are ϕ -dependent scaling factors.

Plateau values of $\Delta(t, t_W)$ and $\Delta_{AB}(t)$ can also be calculated on the assumption that no disk crosses the channel, so that in Eq. (1), $y_i(t+t_W)$ and $y_i(t_W)$ take the same sign; similarly, $y_{A,i}(t)$ and $y_{B,i}(t)$ take the same sign in Eq. (2). Then, on the plateau, $\Delta(t, t_W)$ and $\Delta_{AB}(t)$ can be approximated by

$$\Delta(t, t_W) = \Delta_{AB}(t) \approx 2(\langle y^2 \rangle - \langle |y| \rangle^2). \quad (3)$$

We calculate $\langle y^2 \rangle$ and $\langle |y| \rangle^2$ using the transfer-matrix method of Ref. [16]; the results from Eq. (3) are indistinguishable from the plateau values of Δ and Δ_{AB} seen in Fig. 3.

In recent work, Scalliet et al. [26] have shown that a splitting of the plateau values of Δ and Δ_{AB} is not of itself sufficient to show that there is a state-following Gardner transition that requires the stable glass to split into marginally-stable sub-basins where the two copies A and B sometimes end up. The split can instead be due to a small subset of the particles being frozen into slightly different locations in the two copies. As we shall see, an explanation of this kind also applies to our system of disks in a channel.

For very large times, $t \gg \tau_\alpha$, disks may cross the channel, so that $\langle y_i(t+t_W)y_i(t_W) \rangle \rightarrow 0$; thus, $\Delta(t, t_W)$ and $\Delta_{AB}(t)$ will both reach a *second* plateau at the equilibrium value, $2\langle y_i^2 \rangle \approx h^2/2$. However, this long-time limit is not relevant to the state-following Gardner transition, where one is interested in times such that $\Delta(t, t_W)$ and $\Delta_{AB}(t)$ are still on their first plateau. At the α relaxation time disks begin to escape their cages by crossing from one side of the channel to the other. Channel crossing is strongly suppressed in the absence of defects; thus, for a system with no defects there can be no splitting in the first plateau values of Δ and Δ_{AB} at large packing fractions; this is confirmed by the results shown in Fig. 3. When defects are present, Δ_{AB} and Δ separate, as shown in Fig. 4.

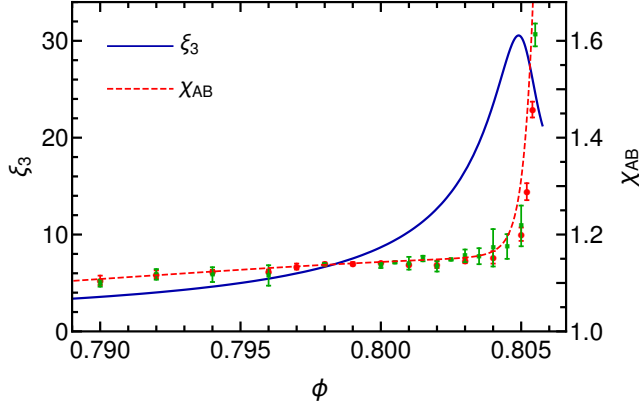


FIG. 6. (Color online) The correlation length ξ_3 as a function of the packing fraction ϕ , and the susceptibility χ_{AB} , calculated using the transfer matrix procedure. Data points show values of χ_{AB} obtained in quenches from a state with no defects, starting from $\phi_i = 0.76$ (red circles) and $\phi_i = 0.78$ (green squares).

To understand the cause of the splitting we turn to the histograms of the plateau values of Δ and Δ_{AB} in Fig. 5. In all cases, one can see that the distribution of Δ_{AB} has acquired additional peaks compared to the distribution for Δ . These arise because, during the quench from ϕ_i to ϕ , in some of the copies of the system one or more disks belonging to defects have managed to escape their cages and have crossed to the other side of the channel. The splitting of the peaks due to channel crossing would be approximately h^2/N , which is consistent with the data in Fig. 5. It should be understood that this process is possible even though the compression time is much shorter than τ_α : Fig. 5 shows that disks have crossed in only a few of the copies of the system, despite the presence of ~ 10 defects in each copy. Our explanation of why there is a splitting of Δ and Δ_{AB} does not invoke a Gardner transition and is similar to that given in Ref. [26] for soft spheres, except that in our system we can explicitly identify the localized defects associated with the disks that move.

Nevertheless, evidence for an avoided Gardner transition in our hard-disk system can be found by studying the appropriate correlation length. Following Ref. [12], we define this from the large-distance behavior of the correlation function associated with $\Delta_{AB}^i = (y_{A,i} - y_{B,i})^2$, i.e., $G_P^0(k) = \langle u_i u_{i+k} \rangle$, where $u_i = \Delta_{AB}^i / \Delta_{AB} - 1$ and Δ_{AB} is the value on the plateau which is given by Eq. (3). For our system of disks moving in a narrow channel, $G_P^0(k)$ can be obtained from a transfer-matrix calculation in the high-density regime where channel crossing can be ignored [33].

The correlation function shows a complicated behavior for small separations k , but for large k it decreases

exponentially as $G_P^0(k) \sim (-1)^k \exp[-k/\xi_3]$. In Fig. 6 we show how the correlation length ξ_3 depends on the packing fraction ϕ . The length scale ξ_3 (which can also be calculated from the eigenvalues of the transfer matrix [16, 33]) rises to its maximum value at $\phi = 0.8049$ before falling again. Such behavior is typical of an avoided transition. Expressed as a distance, $\xi_3 L/N \approx 0.50 \xi_3 \sigma$, the maximum value of the correlation length is approximately 15σ .

The susceptibility χ_{AB} is defined, following Ref. [26], as $\chi_{AB} = N \text{var}(\Delta_{AB}) / \text{var}(\Delta_{AB}^i)$, which is equivalent to

$$\chi_{AB} = \frac{\Delta_{AB}^2}{\text{var}(\Delta_{AB}^i)} \sum_{k=-\infty}^{\infty} G_P^0(k). \quad (4)$$

Figure 6 shows that χ_{AB} grows rapidly as the density increases, with no sign of levelling off as might have been expected for an avoided transition. This is because the sum in Eq. (4) is dominated by the small k region (see the Supplemental Material [33]).

To summarize, the splitting between the plateau values of Δ and Δ_{AB} does not provide strong evidence for a Gardner transition, as it is an artifact that arises when there is a significant chance that a disk will escape its cage during the quench. A similar explanation may apply to the observations reported in Refs. [12, 13]. Our study of the correlation length ξ_3 shows that the Gardner transition is an avoided transition for our one-dimensional system of hard disks. The large magnitude of the correlation length at the avoided transition suggests that for hard spheres in three dimensions the equivalent length scale could be very large; thus we anticipate that it will be challenging for simulations to distinguish an avoided Gardner transition from a true phase transition. Nevertheless, we expect the Gardner transition to be an avoided transition for any potential, hard or soft, in dimensions $d \leq 6$.

ACKNOWLEDGMENTS

We should like to thank Ludovic Berthier and Francesco Zamponi for sharing their insights.

Supplemental Material

This document provides information on how the transfer-matrix method of equilibrium statistical physics [27] can be used to calculate some non-equilibrium properties of a system of confined hard disks. In Sec. I we explain how the timescale for α relaxation can be estimated and in Secs. II and III we show that the correlation function $G_P^0(k)$ and the related susceptibility χ_{AB} can be approximated by making use of correlation functions calculated for a single copy of the system.

I. TIMESCALE FOR α RELAXATION

For our system, the α relaxation time τ_α is determined by the motion of defects; that is, the length of the plateau in $\Delta(t, t_W)$ is the typical time a disk that forms part of a defect waits before crossing the channel. We estimate the timescale for this activated process from

$$\tau_\alpha = \tau_0 e^{\beta \Delta U_d}, \quad (5)$$

where β is the reciprocal temperature, ΔU_d is the height of the free energy barrier, τ_0 is a microscopic timescale of order d_w/v_{rms} , d_w is the average distance of a disk from the wall, and v_{rms} is the root-mean-squared speed of the disks. We obtain an effective potential $U_d(y)$ from the distribution function for the coordinate y_2 of a disk that is part of a defect, so that its neighbors at y_1 and y_3 lie near opposite sides of the channel; that is,

$$\rho_d(y_2) \propto e^{-\beta U_d(y_2)}, \quad (6)$$

where the distribution of y_2 is given by

$$\rho_d(y_2) = A \int_0^{h/2} \int_{-h/2}^0 \rho(y_1, y_2, y_3) dy_1 dy_3. \quad (7)$$

In Eq. (7), $\rho(y_1, y_2, y_3)$ is the 3-disk distribution function, calculated using the transfer matrix method of Ref. [16], and A is a normalization constant, independent of y_2 . Figure 7 illustrates the form of $U_d(y_2)$ found in this way. We estimate the barrier height ΔU_d from $\Delta U_d = U_d(0) - U_d(h/2 - d_w)$. For $\phi = 0.720$ and 0.745 , we find $\tau_\alpha \approx 5$ and 35 , respectively: these values are consistent with the molecular-dynamics results shown in Fig. 2. For $\phi = 0.772$ we obtain $\tau_\alpha \approx 6900$, which is greater than observation time in Fig. 2.

II. SPATIAL CORRELATIONS

The correlation function $G_P^0(k)$ is defined in terms of the relative fluctuations of $\Delta_{AB}^i \equiv (y_{A,i} - y_{B,i})^2$ away from their average value on the plateau, which in this Section we denote simply by Δ_{AB} ; i.e.,

$$G_P^0(k) = \langle u_i u_{i+k} \rangle, \quad (8)$$

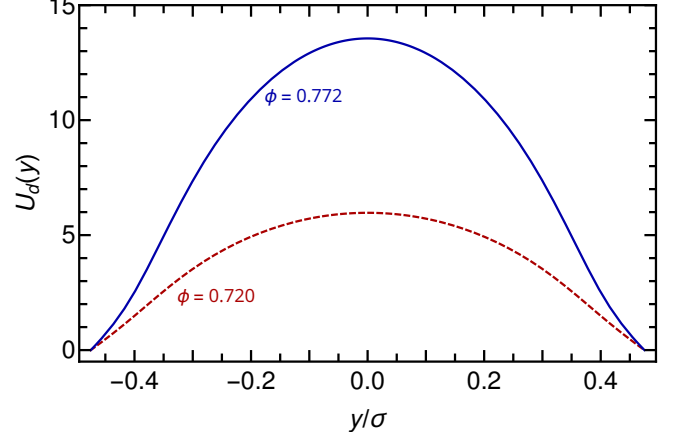


FIG. 7. Free energy $U_d(y)$ of a disk that forms part of a defect as a function of its coordinate y . Results, calculated from Eqs. (6) and (7) with $\beta = 1$ and $h = 0.95\sigma$, are shown for two values of the packing fraction, $\phi = 0.720$ and 0.772 . The height of the barrier increases with ϕ , which leads to the large increase in the timescale τ_α reported in the text.

where $u_i = (\Delta_{AB}^i - \Delta_{AB})/\Delta_{AB}$. In Eq. (8), the average is over many different initial positions for the disks, such that $y_{A,i}(t=0) = y_{B,i}(t=0)$.

The long correlation length for zigzag order and the long relaxation times at high packing fractions allow the two-copy correlation function to be approximated by using results from a single-copy transfer-matrix calculation. The method we use is a straightforward extension of that described in the main text, where it is argued that the plateau value of $\Delta_{AB}(t)$ can be approximated by $2(\langle y^2 \rangle - \langle |y| \rangle^2)$, the average being taken with respect to the equilibrium state of a single copy.

For times t that are small compared with the channel-crossing time τ_α , the signs of $y_{A,i}(t)$ and $y_{B,j}(t)$ are determined by the pattern of defects in the zigzag order, which is the same in each copy. We suppose that if the time is large compared with the β relaxation time τ_β , $y_{A,i}(t)$ and $y_{B,j}(t)$ will be statistically independent, apart from their definite sign relation; naturally, this requires the relevant timescales to be well separated, such that $\tau_\beta \ll t \ll \tau_\alpha$. Thus, a term such as $\langle y_{A,i}^2 y_{A,i+k} y_{B,i+k} \rangle$, which arises in the expansion of $G_P(k)$, can be replaced by $\langle y_{A,i}^2 |y_{A,i+k}| \rangle \langle |y_{B,i+k}| \rangle \equiv \langle y_i^2 |y_{i+k}| \rangle \langle |y_{i+k}| \rangle$, in which the copy labels A and B can be omitted, as the averages are the same for each copy. The final simplification is to approximate each single-copy average by an average over the translationally-invariant equilibrium state, so that $\langle y_i^2 |y_{i+k}| \rangle \langle |y_{i+k}| \rangle \approx \langle y_0^2 |y_k| \rangle \langle |y| \rangle$. We expect this approximation to work well at high density, where the spacing between defects is very large.

By applying the method outlined above, we find

$$G_P(k) \approx \{2\langle y_0^2 y_k^2 \rangle + 4\langle |y_0| |y_k| \rangle^2 - 8\langle y_0^2 |y_k| \rangle \langle |y| \rangle + 2\langle y^2 \rangle^2\} / \Delta_{AB}^2 - 1, \quad (9)$$

which depends on correlation functions of the form $\langle |y_0|^m |y_k|^n \rangle$. Equilibrium correlation functions are calculated from the transfer matrix by the method discussed in Sec. V of Ref. [16] (described there for the case $k = 1$) and in Sec. 2.2 of Ref. [27] (for the one-dimensional Ising model). Results from this calculation are shown in Fig. 8 for a case where the packing fraction is large, $\phi = 0.8058$.

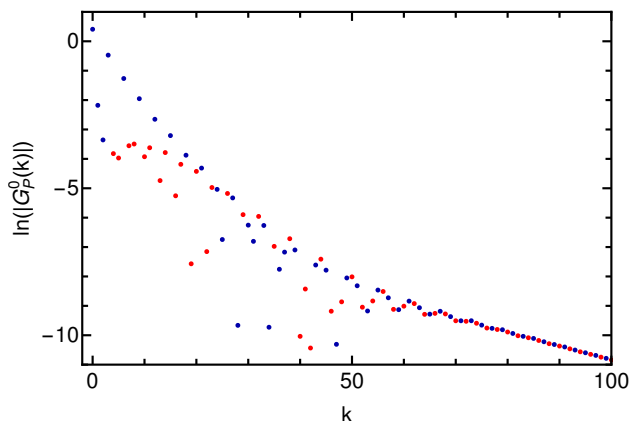


FIG. 8. The correlation function $G_P^0(k)$ as a function of disk separation k at a packing fraction $\phi = 0.8058$. Blue dots indicate that $G_P^0(k)$ is positive, red dots that it is negative. The non-monotonic decrease of $|G_P^0(k)|$ for small k is due to short-ranged crystalline correlations. For large k , the gradient of this log-linear plot is $-1/\xi_3$, which gives the correlation length $\xi_3 \simeq 21$.

Figure 8 show that the correlation function $G_P^0(k)$ decays rapidly as k increases. For $k < 50$ this decay is non-exponential and non-monotonic, owing to the presence of decaying, period-3 oscillations; this can be seen most clearly for $k \leq 18$, where a relatively large, positive value of G_P^0 is always followed by two somewhat smaller values of either sign. Short-ranged crystalline correlations of this kind have been discussed in Ref. [16].

For sufficiently large separations, $k > 70$, the decay of G_P^0 is approximated well by an exponential, $G_P^0(k) \sim (-1)^k \exp[-k/\xi_3]$, which allows us to extract the correlation length ξ_3 . (A similar method has been used in the Supplement to Ref. [12], where a closely-related correlation length ξ_P was calculated for a system of hard spheres.) For our system of disks in a channel, we find that ξ_3 is the same correlation length that determines the decay of correlations between the x -separations of

nearest-neighbor pairs of disks,

$\langle (x_{i+1} - x_i)(x_{i+k+1} - x_{i+k}) \rangle_c \sim (-1)^k e^{-k/\xi_3}$, (10) as described in Ref. [16]. This asymptotic form is, in fact, generic for the correlations between even functions of the variables y_i , because the eigenfunction corresponding to the third-largest eigenvalue, λ_3 , has the same (even) parity as the eigenfunction with the largest eigenvalue, λ_1 . The right-hand side of (10) is identical to $(\lambda_3/\lambda_1)^k$, so that the lengthscale ξ_3 can be calculated directly from the largest and third-largest eigenvalues of the transfer matrix [16]; the alternating sign of the correlation function for large k follows from the fact that λ_3 is negative. As ϕ increases, ξ_3 rises to its maximum value at a packing fraction 0.8049 before falling again, as shown in Fig. [7] of the main text. Thus, if the growth of the correlation length ξ_3 indicates the approach to the Gardner transition, this transition is avoided, as one should expect for a one-dimensional system.

III. SUSCEPTIBILITY χ_{AB}

In Ref. [26], Scalliet *et al.* have defined a susceptibility $\chi_{AB} = N \text{var}(\Delta_{AB}) / \text{var}(\Delta_{AB}^i)$, in which all quantities are evaluated on the plateau in $\Delta_{AB}(t)$. It is straightforward to verify that this definition is equivalent, in our problem, to

$$\chi_{AB} = \frac{\Delta_{AB}^2}{\text{var}(\Delta_{AB}^i)} \sum_{k=-\infty}^{\infty} G_P^0(k). \quad (11)$$

The prefactor ensures that $\chi_{AB} \rightarrow 1$ in the absence of spatial correlations [26]. The plateau value of the denominator $\text{var}(\Delta_{AB}^i)$ can be approximated by the same method that we used to find the plateau value of Δ_{AB} ; we find

$$\begin{aligned} \text{var}(\Delta_{AB}^i) &\approx 2\langle y^4 \rangle + 2\langle y^2 \rangle^2 - 8\langle |y|^3 \rangle \langle |y| \rangle \\ &\quad + 8\langle y^2 \rangle \langle |y| \rangle^2 - 4\langle |y| \rangle^4. \end{aligned} \quad (12)$$

As can be seen from Fig. 7 of the main text, the results of molecular dynamics simulations agree well with the calculated susceptibility, and provide support for the approximations made for the correlation functions in Sec. II. We note from Fig. 7 that χ_{AB} grows rapidly as the packing fraction increases through $\phi = 0.8049$, the position of the maximum in the correlation length ξ_3 . Our definition of the correlation length is unambiguous, but it will be noticed from Fig. 8 that $G_P^0(k)$ is very small in the region of k where exponential decay sets in. The terms that contribute most to the sum in Eq. (11) are, in fact, those with small values of k . The behavior of $G_P^0(k)$ for small k is due to several eigenfunctions whose eigenvalues have magnitudes that are less than, but still comparable with, $|\lambda_3|$; these include the complex eigenvalues that are responsible for the period-3 oscillations noted earlier, in Sec. II.

-
- [1] P. Charbonneau, J. Kurchan, G. Parisi, P. Urbani, and F. Zamponi, “Glass and jamming transitions: From exact results to finite-dimensional descriptions,” *Annu. Rev. Condens. Matter Phys.* **8**, 265 (2017).
- [2] B. Seoane, D. R. Reid, J. J. de Pablo, and F. Zamponi, “Low-temperature anomalies of a vapor deposited glass,” (2017), [arXiv:1709.04930 \[cond-mat.soft\]](https://arxiv.org/abs/1709.04930).
- [3] Pierfrancesco Urbani and Giulio Biroli, “Gardner transition in finite dimensions,” *Phys. Rev. B* **91**, 100202 (2015).
- [4] Patrick Charbonneau, Yuliang Jin, Giorgio Parisi, Corrado Rainone, Beatriz Seoane, and Francesco Zamponi, “Numerical detection of the Gardner transition in a mean-field glass former,” *Phys. Rev. E* **92**, 012316 (2015).
- [5] M. A. Moore and A. J. Bray, “Disappearance of the de Almeida-Thouless line in six dimensions,” *Phys. Rev. B* **83**, 224408 (2011).
- [6] Wenlong Wang, M. A. Moore, and Helmut G. Katzgraber, “Fractal dimension of interfaces in Edwards-Anderson and long-range Ising spin glasses: Determining the applicability of different theoretical descriptions,” *Phys. Rev. Lett.* **119**, 100602 (2017).
- [7] Wenlong Wang, M. A. Moore, and Helmut G. Katzgraber, “Fractal dimension of interfaces in Edwards-Anderson spin glasses for up to six space dimensions,” (2017), [arXiv:1712.04971 \[cond-mat.dis-nn\]](https://arxiv.org/abs/1712.04971).
- [8] J. Mattsson, T. Jonsson, P. Nordblad, H. Aruga Katori, and A. Ito, “No Phase Transition in a Magnetic Field in the Ising Spin Glass $\text{Fe}_{0.5}\text{Mn}_{0.5}\text{TiO}_3$,” *Phys. Rev. Lett.* **74**, 4305 (1995).
- [9] T. Jörg, H. G. Katzgraber, and F. Krzakala, “Behavior of Ising Spin Glasses in a Magnetic Field,” *Phys. Rev. Lett.* **100**, 197202 (2008).
- [10] M. Baity-Jesi, R. A. Baños, A. Cruz, L. A. Fernandez, J. M. Gil-Narvion, A. Gordillo-Guerrero, D. Iñiguez, A. Maiorano, F. Mantovani, E. Marinari, V. Martin-Mayor, J. Monforte-Garcia, A. Muñoz Sudupe, D. Navarro, G. Parisi, S. Perez-Gaviro, M. Pivanti, F. Ricci-Tersenghi, J. J. Ruiz-Lorenzo, S. F. Schifano, B. Seoane, A. Tarancon, R. Tripiccion, and D. Yllanes, “Dynamical transition in the $D = 3$ Edwards-Anderson spin glass in an external magnetic field,” *Phys. Rev. E* **89**, 032140 (2014).
- [11] M. Baity-Jesi and Janus collaboration, “The three-dimensional Ising spin glass in a field: The role of the silent majority,” *J. Stat. Mech.* **2014**, P05014 (2014).
- [12] L. Berthier, Patrick Charbonneau, Yuliang Jin, Giorgio Parisi, Beatriz Seoane, and Francesco Zamponi, “Growing timescales and lengthscales characterizing vibrations of amorphous solids,” *PNAS* **113**, 8397 (2016).
- [13] A. Seguin and O. Dauchot, “Experimental evidence of the Gardner phase in a granular glass,” *Phys. Rev. Lett.* **117**, 228001 (2016).
- [14] Corey O’Hern, “Signs of a Gardner transition in a granular glass,” *Physics* **9**, 133 (2016).
- [15] J. F. Robinson, M. J. Godfrey, and M. A. Moore, “Glasslike behavior of a hard-disk fluid confined to a narrow channel,” *Phys. Rev. E* **93**, 032101 (2016).
- [16] M. J. Godfrey and M. A. Moore, “Understanding the ideal glass transition: Lessons from an equilibrium study of hard disks in a channel,” *Phys. Rev. E* **91**, 022120 (2015).
- [17] M. J. Godfrey and M. A. Moore, “Static and dynamical properties of a hard-disk fluid confined to a narrow channel,” *Phys. Rev. E* **89**, 032111 (2014).
- [18] R. K. Bowles and I. Saika-Voivod, “Landscapes, dynamic heterogeneity, and kinetic facilitation in a simple off-lattice model,” *Phys. Rev. E* **73**, 011503 (2006).
- [19] Mahdi Zaeifi Yamchi, S. S. Ashwin, and Richard K. Bowles, “Fragile-strong fluid crossover and universal relaxation times in a confined hard-disk fluid,” *Phys. Rev. Lett.* **109**, 225701 (2012).
- [20] S. S. Ashwin, Mahdi Zaeifi Yamchi, and Richard K. Bowles, “Inherent structure landscape connection between liquids, granular materials, and the jamming phase diagram,” *Phys. Rev. Lett.* **110**, 145701 (2013).
- [21] Mahdi Zaeifi Yamchi, S. S. Ashwin, and Richard K. Bowles, “Inherent structures, fragility, and jamming: Insights from quasi-one-dimensional hard disks,” *Phys. Rev. E* **91**, 022301 (2015).
- [22] S. S. Ashwin and Richard K. Bowles, “Complete jamming landscape of confined hard discs,” *Phys. Rev. Lett.* **102**, 235701 (2009).
- [23] D. A. Kofke and A. J. Post, “Hard particles in narrow pores. Transfer matrix solution and the periodic narrow box,” *J. Chem. Phys.* **98**, 4853 (1993).
- [24] S. Varga, G. Ball, and P. Gurin, “Structural properties of hard disks in a narrow tube,” *Journal of Statistical Mechanics: Theory and Experiment* **2011**, P11006.
- [25] P. Gurin and S. Varga, “Pair correlation functions of two- and three-dimensional hard-core fluids confined into narrow pores: Exact results from transfer matrix method,” *J. Chem. Phys.* **139**, 244708 (2013).
- [26] C. Scalliet, L. Berthier, and F. Zamponi, “Absence of marginal stability in a structural glass,” *Phys. Rev. Lett.* **119**, 205501 (2017).
- [27] R. J. Baxter, *Exactly Solved Models in Statistical Mechanics* (Academic Press, 1982).
- [28] M. Wyart and M. E. Cates, “Does a growing static length scale control the glass transition?” *Phys. Rev. Lett.* **119**, 195501 (2017).
- [29] Aaron S. Keys, Lester O. Hedges, Juan P. Garrahan, Sharon C. Glotzer, and David Chandler, “Excitations are localized and relaxation is hierarchical in glass-forming liquids,” *Phys. Rev. X* **1**, 021013 (2011).
- [30] F. Ritort and P. Sollich, “Glassy dynamics of kinetically constrained models,” *Advances in Physics* **52**, 219 (2003).
- [31] Frank H. Stillinger, “Supercooled liquids, glass transitions, and the Kauzmann paradox,” *J. Chem. Phys.* **88**, 7818 (1988).
- [32] Boris D. Lubachevsky and Frank H. Stillinger, “Geometric properties of random disk packings,” *Journal of Statistical Physics* **60**, 561–583 (1990).
- [33] See Supplemental Material at [URL will be inserted by publisher] for explanations of how the transfer-matrix method was used to obtain approximate results for τ_α , $G_P^0(k)$, and χ_{AB} .